Journal Pre-proof

Modified Shoutai Pill inhibited ferroptosis to alleviate recurrent pregnancy loss

Yuling Lai, Yu Zhang, Huimin Zhang, Zhenyue Chen, Lihua Zeng, Gaopi Deng, Songping Luo, Jie Gao

PII: S0378-8741(23)00896-6

DOI: https://doi.org/10.1016/j.jep.2023.117028

Reference: JEP 117028

To appear in: *Journal of Ethnopharmacology*

Received Date: 21 June 2023

Revised Date: 1 August 2023

Accepted Date: 9 August 2023

Please cite this article as: Lai, Y., Zhang, Y., Zhang, H., Chen, Z., Zeng, L., Deng, G., Luo, S., Gao, J., Modified Shoutai Pill inhibited ferroptosis to alleviate recurrent pregnancy loss, *Journal of Ethnopharmacology* (2023), doi: https://doi.org/10.1016/j.jep.2023.117028.

Credit Author Statement

Yuling Lai:Conceptualization, Methodology,Writing- Original draft preparation. Yu Zhang and Huimin Zhang:Validation, Visualization. Zhenyue Chen and Lihua Zeng:Validation. Gaopi Deng:Supervision. Songping Luo and Jie Gao:Conceptualization,Writing- Reviewing and Editing.

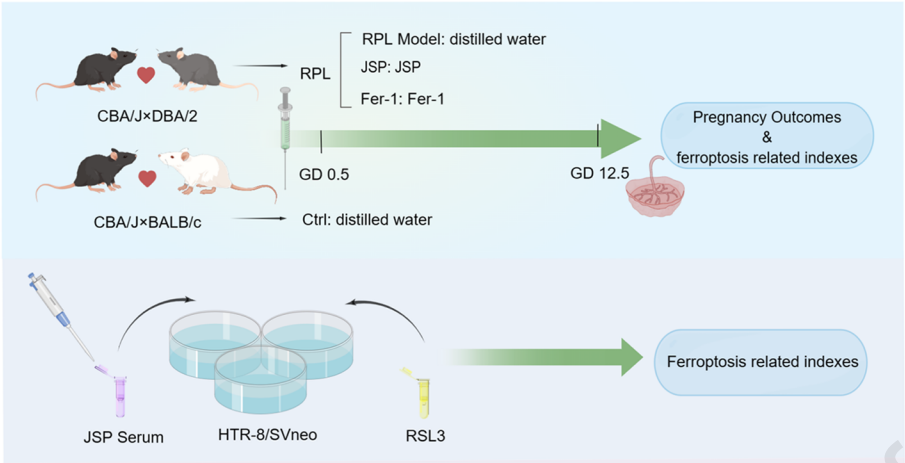

Conclusions: JSP could treat RPL through inhibiting ferroptosis.

Modified Shoutai Pill Inhibited Ferroptosis to Alleviate Recurrent Pregnancy Loss

Yuling Lai[1,2], Yu Zhang[1], Huimin Zhang[1], Zhenyue Chen[1], Lihua Zeng[1], Gaopi Deng[3], Songping Luo[3*], Jie Gao[3*]

[1]Guangzhou University of Chinese Medicine, Guangzhou, 510405, People's Republic of China

[2]Guangzhou Sport University, Guangzhou, 510500, People's Republic of China

[3]The First Affiliated Hospital of Guangzhou University of Chinese Medicine, Guangzhou, 510405, People's Republic of China

[*]Correspondence:

Jie Gao: The First Affiliated Hospital of Guangzhou University of Chinese Medicine, Guangzhou, 510405, gaojie1769@gzucm.edu.cn and Songping Luo: The First Affiliated Hospital of Guangzhou University of Chinese Medicine, Guangzhou, 510405, songpingluo@hotmail.com.

Abstract

Ethnopharmacological relevance: Modified Shoutai Pill, also called Jianwei Shoutai Pill (JSP), is a traditional Chinese medicine prescription that has been used as an effective agent for the treatment of miscarriage.

Aim of the study: To explore the potential molecular mechanism of JSP against recurrent pregnancy loss (RPL).

Materials and Methods: *In vivo,* CBA/J mated DBA/2 mice were used to conduct RPL model, while CBA/J mated BALB/c mice were seen as the control group. Mice were orally administered with JSP, Fer-1 (a ferroptosis inhibitor) or distilled water from day 0.5-12.5 of gestation (GD 0.5-12.5). Pregnancy outcomes were analyzed and ferroptosis related indexes of the whole implantation sites were measured on GD 12.5. *In vitro,* human trophoblast cell line HTR-8/SVneo was cultured and treated with RAS-selective lethal small molecule 3 (RSL3) (a ferroptosis agonist) or different

concentrations of JSP. Then, ferroptosis related indexes were tested to analyze whether JSP could inhibit ferroptosis in HTR-8/SVneo cells.

Results: *In vivo* consequences demonstrated that JSP or Fer-1 alleviated pregnancy outcomes including lower resorption rate and abortion rate. In addition, excessive iron accumulation and MDA level were inhibited, while GSH and GPX content were raised under JSP or Fer-1 exposure. Also, JSP or Fer-1 enhanced protein expressions of GPX4 and SLC7A11 which suppress ferroptosis, and lightened protein expression of ACSL4 which boosts ferroptosis. *In vitro,* JSP rescued HTR-8/SVneo cell death and migration ability that were injured by RSL3. Furthermore, JSP inhibited RSL3-induced intracellular reactive oxygen species (ROS), lipid ROS and iron deposition.

Conclusions: Collectively, our findings illustrated that the mechanism of JSP in treating RPL might be related to inhibiting ferroptosis, which provided a novel insight into the application of JSP in RPL intervention.

Keywords: Jianwei Shoutai Pill; pregnancy loss; pregnancy outcomes; ferroptosis.

Abbreviations

ACSL4 (Acyl-CoA synthetase long-chain family member 4); CCK8 (Cell Counting Kit-8); DCFH-DA (Dichlorofluorescin-diacetate); Ferrostatin-1 (Fer-1) ; Ferritin Heavy Chain 1 (FTH1); GPX (glutathione peroxidase); GSH (Glutathione); HTR-8/SVneo (human chorionic trophoblast cell line); Jianwei Shoutai Pill (JSP); LDH (Lactate Dehydrogenase); labile iron pool (LIP); MDA (malondialdehyde); RPL (Recurrent pregnancy loss); ROS (Excessive reactive oxygen species); RSL3 (RAS-selective lethal small molecule 3); SLC7A11(Solute carrier family 7 member 11); Traditional Chinese medicine (TCM)

1. Introduction

Recurrent pregnancy loss (RPL), defined as two or more clinically proven miscarriages

before 20 to 24 weeks of gestation, including loss of embryos and fetuses (Dimitriadis et al 2020). It is a distressing pregnancy disorder that affects about 2.5 percent of women trying to conceive (El Hachem et al 2017). The risk of RPL increases with the number of pregnancy losses, which include maternal age, previous number of miscarriages, anti- phospholipid syndrome, uterine malformation, chronic endometritis and impaired decidualization, overt hypothyroidism, abnormal parental karyotypes, obesity (BMI >30 kg/m^2) and lifestyle factors (stress, smoking and excessive alcohol consumption)(Amer 2012; Atik et al 2018). Specifically, 50-70% of couples have no clear risk factors for RPL (Dimitriadis et al 2020; Jaslow et al 2010; Morita et al 2019). Recent studies have highlighted the role of over activation of placental reactive oxygen species (ROS) in the pathogenesis of RPL (Al-Sheikh et al 2019). A study found that the levels of oxidative stress markers (malondialdehyde (MDA), H_2O_2) in plasma and placenta of RPL patients were increased, while the levels of enzymatic antioxidants (GPX, SOD, CAT) were decreased, suggesting that oxidative stress is an important pathogenic factor of RPL (Al-Sheikh et al 2019).

Ferroptosis is a unique iron-dependent form of nonapoptotic cell death, driven by the excessive accumulation of peroxidized lipids (Dixon et al 2012). Ferroptosis involves overload Fe^{2+} concentration, lethal cell membrane lipid peroxidation and failure of GSH-dependent antioxidant defense that caused by GPX4 inactivation(Koppula et al 2021). During pregnancy, the importance of iron intake to support growth and development of the fetus is well known. However, recent studies have suggested that consuming excessive iron may paradoxically increase the odds of reproductive disorders (Brannon & Taylor 2017; Fisher & Nemeth 2017). For example, disorders related to iron dysregulation are associated with placental dysfunction in preeclampsia (Fisher & Nemeth 2017; Lee et al 2011; Vaughan & Walsh 2002). Moreover, excessive lipid peroxidation is associated with several pathways of cell death (Su et al 2019), particularly in ferroptosis, lipid peroxidative activity, which is LOX-dependent in the presence of iron is present (Shintoku et al 2017). Evidences suggest that placental and systemic oxidative stress may play a role in the pathogenesis of adverse pregnancy such

as threatened pregnancy loss and preeclampsia (Aouache et al 2018; Ferguson et al 2017; Taravati & Tohidi 2018; Vaka et al 2018). A study reported that the accumulation of lipid peroxidation exerted inhibitory effects on various cellular functions of trophoblasts, including the invasion and migration (Yang et al 2018). In another study, spontaneous preterm birth was linked to GPX4 inhibition which further caused primary ferroptosis and damage to trophoblasts in mice (Beharier et al 2020). Besides, another study (Zhang et al 2020) showed that ferroptosis occurred in the placental tissue of preeclampsia patients and ferroptosis inhibitor increased trophoblast viability to ameliorate preeclampsia symptoms in a rat model. However, whether ferroptosis involved in the pathogenesis of RPL reminds elusive.

Treatment of RPL is another challenge that puzzles clinicians, and the evidence-based practice in RPL is still not feasible (Sadeghi 2016). To date, various therapeutic strategies, including immunologic intervention, anticoagulant therapy, hormonal supplementation and microelement supplementations have been applied to improve pregnancy outcomes of RPL patients, but no effective therapy has been confirmed. Traditional Chinese medicine (TCM) has been widely used in China and other Asian countries for centuries. According to the TCM theory, the pathogenesis of RPL is always dominated by kidney deficiency. Zhang Xichun, a famo us TCM physician in the Qing Dynasty, invented Shoutai Pills which is composed of *Cuscuta chinensis* Lam (*Tu-Si-Zi*), *Dipsacus* L. (*Xu-Duan*), *Taxillus sutchuenensis* var. *duclouxii* (Lecomte) H.S.Kiu (*Sang-Ji-Sheng*) and Donkey-hide Glue as a classical herbal prescription for invigorating the kidney and relieving pregnancy loss(Zhang et al 2023). Shoutai Pills has been reported to change the bias of TH1/TH2 cytokines to TH2, thereby inducing maternal-fetal immune tolerance (Lai et al 2010). Also, a study indicated that Shoutai Pill containing serum could enhance the proliferation, invasion and migration abilities of trophoblasts and stimulate β-hCG secretion, which may be one of the mechanisms that Shoutai Pill prevents and treats pregnancy loss (Li et al 2016). In addition, another research demonstrated that Shoutai Pill could regulate serum immune factors and perform immunomodulation on pregnant rats exposed to di (2-ethylhexyl) phthalate

(DEHP) by antagonizing the estrogen-like effect of DEHP (Jin et al 2020). Jianwei Shoutai Pill (JSP) (*Cuscuta chinensis* Lam, *Taxillus sutchuenensis* var. *duclouxii* (Lecomte) H.S.Kiu and *Dipsacus* L.), deleted with asini corii colla in a fixed dosage ratio, could be recognized as Modified Shoutai Pill. In the previous study, JSP was obtained through clinical-animal experiment-special software simulation calculation-experimental verification and the drug compatibility rule was conducted by uniform design. The practice has proved that Jianwei Shoutai Pill has the same effect as Shoutai Pill for invigorating the kidney and relieving the miscarriage (Yuexi et al 2021). Nevertheless, the underlying mechanism by which JSP prevents RPL is still elusive.

With the combined application of TCM and modern biomedical technologies, the relationship between the essence of kidney deficiency and lipid peroxidation has been discussed. Studies have reported that when kidney deficiency occurs, the contents of lipid peroxide increase, the activities of antioxidant enzymes decrease and the biological characteristics of the cell membrane are abnormal. Ferroptosis is mainly characterized by the failure of the GSH antioxidant mechanism and the accumulation of lipid peroxide. JSP has the effect of tonifying the kidney, but its regulatory mechanism on ferroptosis has not been reported.

Therefore, this study intends to explore the pathological relationship between ferroptosis and RPL, and to study whether JSP regulates ferroptosis to cure RPL by constructing RPL mouse model and trophoblast ferroptosis model.

2. Materials and methods

2.1. Chemicals and reagents

RSL3 (S8155) and Ferrostatin-1 (Fer-1) (S7243) were purchased from Selleck (USA). Glutathione peroxidase 4 (GPX4, ab125066), Recombinant Solute Carrier Family 7, Member 11 (SLC7A11, ab175186), and Ferritin Heavy Chain 1 (FTH1) (ab89787) were provided by Abcam (England). GAPDH (10491-1-AP), horseradish peroxidase-conjugated goat anti-rabbit IgG (SA00001-2) and acyl-CoA synthetase long-chain family member 4 (ACSL4, ab155282) were obtained from Proteintech (China).

2.2. Preparation and quality control of Decoction and medicated serum of JSP

2.2.1. Decoction of JSP

JSP is composed of *Cuscuta chinensis* Lam, *Taxillus sutchuenensis* var. *duclouxii* (Lecomte) H.S.Kiu and *Dipsacus* L. **(Table 1)**. The Jianwei Shoutai Pill solution was prepared in the ratio of 4：3：3. Qualified *Cuscuta chinensis* Lam, *Taxillus sutchuenensis* var. *duclouxii* (Lecomte) H.S.Kiu and *Dipsacus* L. were screened and were fed to mice according to 20 g： 15 g：15g. Then herbs were decocted with 10 times the amount of water for 1 hour, then decocted with 8 times the amount of water for 1 h. To combine the filtrate and to freeze dry it for 24 h into powder after concentration. The lyophilized powder was dissolved in distilled water to prepare JSP solution, and the solution was stored at 4 ℃ for standby.

Table 1

Names and ratios of three constituent herbs in JSP

Chinese name	Botanical* name	Genus family	English name	Weight (g)	Part used	Batch number	Herb-producing region
Sang-Ji-Sheng	*Taxillus sutchuenensis* var. *duclouxii* (Lecomte) H.S.Kiu	*Loranthaceae*	*Herba Taxilli*	15	Stem	160601	Guangdong
Xu-Duan	*Dipsacus* L.	*Caprifoliaceae*	*Dipsaci Radix*	15	Dried root	140705511	Guangdong
Tu-Si-Zi	*Cuscuta chinensis* Lam	*Convolvulaceae*	*Cuscutae Semen*	20	Seed	150701	Guangdong

* The plant name has been checked with http://www.worldfloraonline.org. Accessed on: 06 Jun 2023'.

2.2.2. Medicated Serum of JSP

Twenty SPF male SD rats were randomly divided into control group (gavage with the same amount of normal saline) and JSP group (gavage with the dose of 8.2g/kg/d). Rats were gavaged once a day for 7 days. One hour after the last administration, the rats were anesthetized with mixed ratio of zoletil and xylazine. Blood was collected through the abdominal aorta and left for more than 4 hours. The serum was separated after blood centrifugation and inactivated with water bath. Then the serum was filtered and sterilized, and stored in the refrigerator at - 20 ℃ for storage.

2.2.3. LC-MS conditions

JSP powder was dissolved in methanol, followed by 30 minutes of ultrasonic shaking at 100 Hz. The supernatant was carefully filtered through a 0.22 μm microporous membrane and stored at -80 °C until ultra-high-performance liquid chromatography (UPLC) -MS analysis. LC-MS/MS analysis was performed using a Waters ACQUITY UPLC system with a Waters UPLC BEH C18 column (1.7 μm, 2.1×100 mm). The flow rate was set at 0.3 mL/min and the sample injection volume at 5 μL. The mobile phase consisted of 0.1% formic acid in water (A) and acetonitrile (B). The following describes the multistep linear elution gradient program: 0–10 min, 95−73% A; 10–12 min, 73−50% A; 12–20 min, 50−0% A; 20–21 min, 0−95% A; 21–22 min, 95% A; A waters Xevo G2-S Q-TOF mass spectrometry was employed to obtain the MS data based on the negative-ion mode. During acquisition cycle, the mass range was from 50 to 1,200. The cone gas flow rate was 50 L/h, the desolvation gas flow rate was 550 L/h and capillary temperature was 100 °C; capillary voltage was 2800 V. Data was analyzed by MassLynx (Version 4.1).

2.3. Animal model and drug treatment

All mice were handled according to the Guide for the Care and Use of Laboratory Animals and all protocols were authorized by the Research Medical Ethics Committee of The First Affiliated Hospital of Guangzhou University of Chinese Medicine (20220520001). The mice were bought from Guangdong Provincial Medical

Laboratory Animal Center (Guangdong, China) (SYXK (Yue) 2020-0229). In this study, female CBA/J mice were mated male BALB/c to establish a normal pregnancy model (control group), and with male DBA/2 mice to develop an RPL group. The beginning of pregnancy was marked by the appearance of vaginal tamponade after sexual intercourse and was considered day 0.5 of gestation (GD 0.5).

Our research team has used high (16.4g/kg), middle (8.2g/kg) and low concentrations (4.1g/kg) of JSP in CBA/J×DBA/2 mice to identify the protective effect of JSP against RPL in previous study(Xiaoli et al 2020). The results showed that abortion rates were reduced in middle dose and low dose of JSP groups, and middle dose of JSP manifested the most obvious effect. Considering that laboratory animals have valued lives and the optimal dose has been determined earlier, we employed a single dose (8.2g/kg) in this study. CBA/J mice in RPL group were orally administered with JSP (8.2 g/(kg·d)) to create the JSP group, while CBA/J mice in control group were given intraperitoneal injections with Fer-1 (5 mg/(kg·d)) to create the Fer-1 group. The control group and RPL group were administered the same volume of distilled water. The medicine was provided from GD 0.5-GD 12.5 in the female mice.

2.4. Sample collection of animal experimentation

The female mice were euthanized through cervical dislocation, followed by observation of vaginal and uterine bleeding, and counting of the number of surviving and resorbed embryos. The abortion embryos exhibited smaller implantation site, necrosis and hemorrhage. The embryo resorption rate = reabsorbed embryos / (surviving embryos+reabsorbed embryos) ×100%. The whole implantation sites (containing decidua and early placenta) were washed in 0.9% saline to remove the blood, then a portion of the sample were stored in cryopreservation tube and stored at –80°C for future analysis, while the remaining tissue were fixed with 4% paraformaldehyde (PFA) for tissue sections.

2.5. Measurement of Glutathione (GSH), glutathione peroxidase (GPX), malondialdehyde (MDA)

Collected tissues or culture supernatants were lysised with radioimmunoprecipitation (RIPA) lysis buffer (Beyotime, China) and washed with PBS. Contents of GSH, GPX and MDA in the cell homogenate were detected using specific kits (Beyotime, China) following the manufacturer's instructions.

2.6. Western blot assay

Tissues or cells were lysed on ice for 20 min using radioimmunoprecipitation (RIPA) buffer (Beyotime, China). Lysates were heated at 100 ℃ for 5 min and quantified using a BCA protein assay kit (Beyotime, China). Then 30 mg proteins were separated by SDS-PAGE gel electrophoresis and transferred to PVDF membrane. Sealing the membranes with 5% non-fat milk for 2 h and incubated overnight at 4℃ with primary antibodies against: GPx4, SLC7A11, ACSL4, FTH1, GAPDH. Membranes were incubated with the anti-rabbit IgG coupled with horseradish peroxidase (HRP) for 1 h. The target bands were detected using ECL regent in a multifunctional imager (Biorad, America) and densitometric analysis was performed by ImageJ software.

2.7. Immunohistochemistry staining and TUNEL staining

After dewaxing and hydration of paraffin sections (5 μm thick), heat-induced antigen retrieval was performed using an EDTA antigen repair solution (Beyotime, China). Then endogenous peroxidase activity was blocked with 3% H_2O_2 for 10 min. The slices were incubated overnight with primary antibodies against: GPx4, SLC7A11, ACSL4, TfR1 and Nrf2 at 4℃. Slices were incubated with secondary antibody for 30 min, followed by 3,3-diaminobenzidine (DAB) (ZSGB-Bio, China) staining and hematoxylin counterstaining. Images were captured under an optical microscope (Olympus, Japan) and Image J software was used for analyzing the histochemistry score.

To analyze apoptosis of placenta tissues in different groups, the terminal deoxynucleotidyl transferase dUTP nick end labeling (TUNEL) staining was conducted according to the manufacturer's instructions (Beyotime, China).

2.8. HTR-8/SVneo culture and treatment

Human trophoblast--HTR-8/SVneo cells were obtained from the American Type Culture Collection (ATCC, USA) and stored in the presence of 10% fetal bovine serum (GIBCO, USA) and anti-biotics (100 μg/mL streptomycin and 100 IU/ml penicillin) in DMEM medium (GIBCO, USA) at 37℃ in a humidified atmosphere containing 5% CO_2. According to our previous study, RSL3 was added to trophoblasts to induce ferroptosis in a concentration of 0.1μM(Lai et al 2022). Cells were divided into 3 groups: control, RSL3 and JSP groups (3 different concentrations of JSP). The control and RSL3 groups received a 10% drug-free serum medium, whereas JSP group received a medium containing 10% rat serum which was composed of 3 different concentrations of JSP (i.e., the complete medium for the 5% JSP group included 5% JSP-containing serum, 5% drug-free serum, 89% DMEM and 1% penicillin-streptomycin). After 24 h, the control group received a complete medium, while the RSL3 and JSP groups received a complete medium containing RSL3 for 24 h.

2.9. CCK-8 assay and cytotoxicity measurement

A cell counting kit-8 (CCK-8) (Dojindo, Japan) was used to assess cell viability. HTR-8/SVneo cells were sown into 96-well plates and treated with different doses of JSP for 24 h and then cultured with 0.1 μM RSL3 after another 24 h. Then 10 μl CCK-8 regent was added to each well and incubated at 37℃ for 4 h. A microplate reader (ELx800, BioTek, USA) was used to measure the optical density at 450 nm.

Cell supernatants were collected. Cytotoxicity was measured by LDH release assay using a kit following the manufacturer's instructions (Beyotime, Shanghai, China).

2.10. Detection of cellular ROS, labile Fe^{2+} contents and lipid ROS

The generation of intracellular ROS was analyzed with a fluorescent DCHF- DA assay kit (Beyotime China) and detecting labile iron pool (LIP) in the cell

homogenate was tested by a FeRhoNox-1 fluorescent probe (MKBio, China) following the manufacturer's instructions.

To detect lipid ROS in the cell membrane, a C11-BODIPY $^{581/591}$ fluorescent probe (ABclonal, China) was used. Cells were seeded into 6-well plates and treated according to different conditions. Then cells were incubated with 50 μm C11-BODIPY $^{581/591}$ for 1 h according to the manufacturer's instructions. Oxidized BODIPY (Ox C11) and non-oxidized BODIPY (Non-Ox C11) were observed at excitation wavelengths of 488 nm and 565 nm under a confocal laser scanning microscope (Leica, Germany).

2.11. Wound healing assay

Cell migration was measured by wound healing assay. HTR-8/SVneo cells were seeded into six-well plates and grown to >90% confluence. To create wounds, cell monolayers were scraped with a pipette tip. After the appropriate treatments, cells were rinsed twice with fresh RPMI-1640 medium and cultured for a further 24 h. The wound area was recorded at 0 h and 24 h under a microscope (Olympus). Migration was recorded as the percentage wound closure at 24 h and analyzed by ImageJ software.

2.12. Statistical analysis

Data were presented as mean ± standard deviation (SD). Statistical significance of the differences was evaluated using SPSS 20.0. Student's t test was employed to compare the means of two groups and one-way analysis of variance (ANOVA) with LSD test or Dunnett's T3 test was applied to compare the means of three or more groups. A statistically significant difference was defined as $P<0.05$.

3. Results

3.1. Both JSP and Fer-1 attenuated pregnancy loss in CBA/J×DBA/2 mice

Firstly, we used the HPLC-MC fingerprint to identify the main chemical compositions

of JSP (**Figure 1)**. Based on the successful preparation of JSP solution with controllable quality, we observed the phenomenon of ferroptosis and the protective effect of JSP in abortion mice. Female CBA/J mice were mated with male DBA/2 mice to create an RPL mouse model, and with male BALB/c mice to achieve a normal pregnancy in this study. The abortion rates were analyzed on GD 12.5 of pregnancy in the control, RPL, JSP, and Fer-1 (a lipophilic radical scavenger) groups. In RPL group, less embryos existed at the implantation site and the arrows presented the fetal reabsorption (**Figure 2A**). As existed description by other researches, the markedly higher abortion rate was observed in the CBA/J×DBA/2 than CBA/J×BALB/c (32.56% versus 5.06%) in our study, which suggested that the RPL mouse model was conducted successfully (**Figure 2B**). Besides, JSP (15.50%) and Fer-1 (15.22%) manifested notably lower abortion rates compared to RPL group (32.56%). Besides, compared with control, JSP and Fer-1 group, the placental weight was remarkably lower in the RPL group (**Figure 2C**). In addition, there is no significant differences in uterus weight, decidual weight and body weight among all the groups (**Figure 2D-F**).

In addition, the apoptosis of placenta was observed by TUNEL staining. In contrast to the control group and JSP group, TUNEL staining revealed a higher rate of apoptosis of placenta in the RPL group (**Figure 2G-H**). These results revealed that placenta development of the RPL mice was possibly limited and JSP obviously reduced abortion rated and inhibited placenta injury.

Interestingly, Fer-1, a classic ferroptosis inhibitors, manifested a similar inhibitory effect on the abortion rate of mice as JSP (**Figure 2C**). Therefore, we continued to collect the evidence of ferroptosis activation and further explored the intervention effect of JSP on ferroptosis in abortion mice.

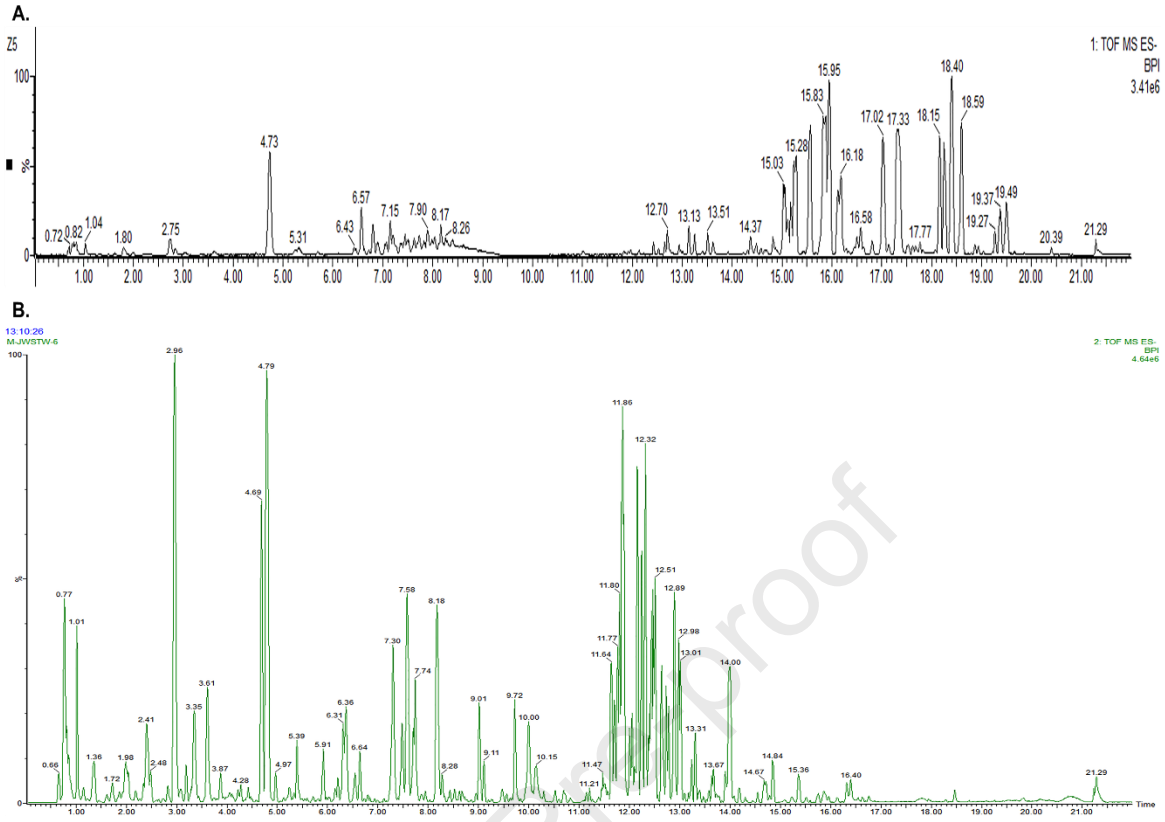

Figure 1. Chemical characterization of JSP drug-containing serum and decoctions using HPLC.

(A) Chemical characterization of mediated serum of JSP. (B) Chemical characterization of JSP decoctions.

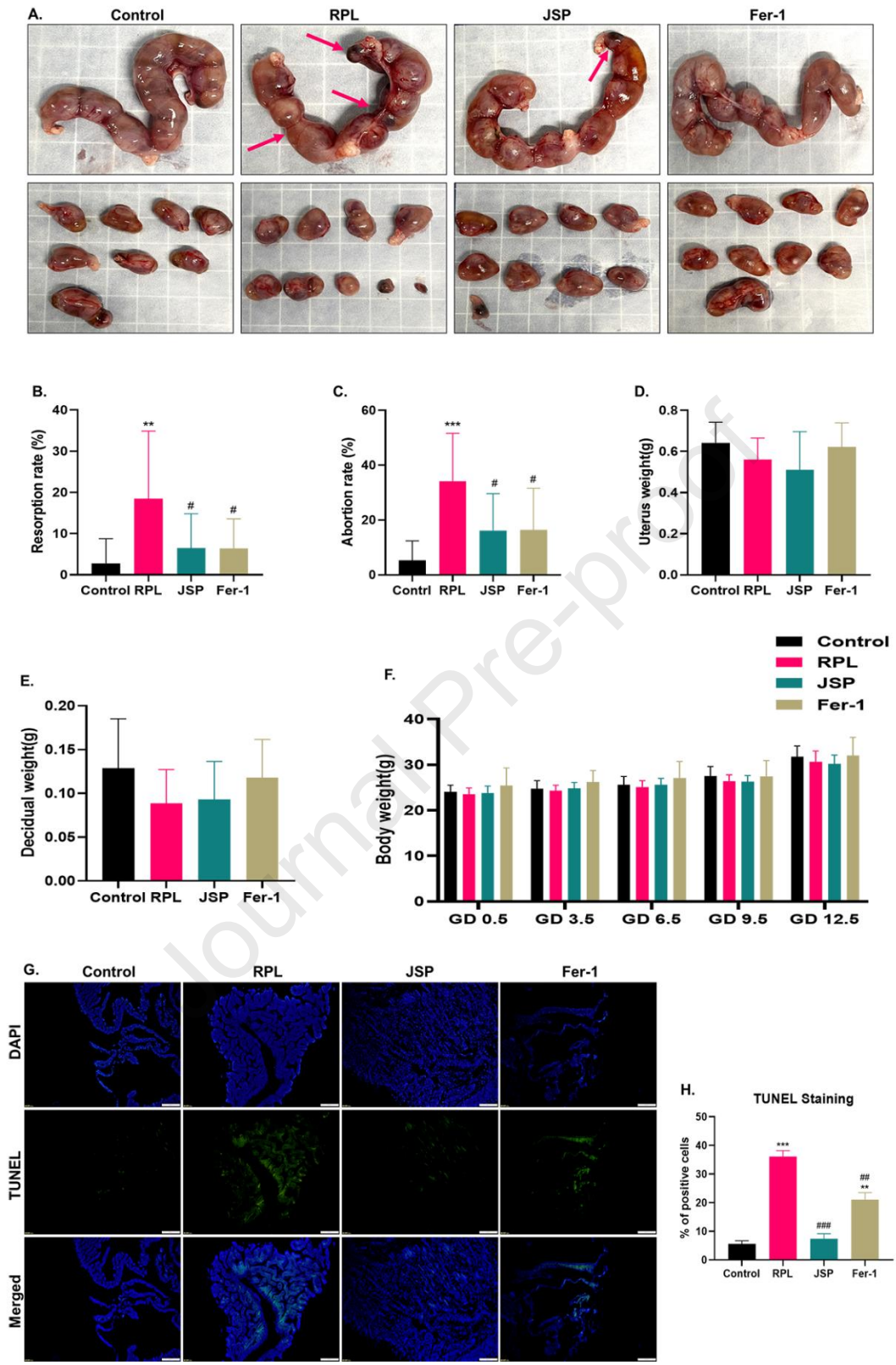

Figure 2. Both JSP and Fer-1 attenuated pregnancy loss in CBA/J×DBA/2 mice

(A) Representative images of embryos in each group. Arrows indicated resorbed embryos. (B) Resorption rate in each group (n = 10 per group). (C) Abortion rate in

each group (n = 10 per group). (D-F) Comparison of uterus weight, decidual weight and body weight in each group (n = 10 per group). G. Representative images of the placenta tissue by TUNEL staining (n =4 per group). (H) Quantification of apoptosis by TUNEL staining. Scale bar: 100 μm. $^{**}P<0.01$, $^{***}P<0.001$, compared with the control group; $^{\#}P<0.05$, $^{\#\#}P<0.01$, $^{\#\#\#}P<0.001$ compared with the RPL group.

3.2. Both JSP and Fer-1 inhibited ferroptosis in RPL mice

Subsequently, we evaluated the anti-lipid peroxidation of JSP and Fer-1 in the implantation sites of pregnant mice. GSH content (**Figure 3A**) and GPX activity (**Figure 3B**) were decreased in RPL group, meanwhile MDA level was increased in RPL group (**Figure 3C**), which indicated that over lipid peroxide was failed to be removed in mice when RPL happens. Besides, both JSP and Fer-1 could raise GSH content, GPX activity and reduce MDA level to inhibit lipid peroxidation in pregnant mice. The Fe^{2+} detection also manifested that both JSP and Fer-1 obviously inhibited excessive iron deposition which was observed in RPL group (**Figure 3D**).

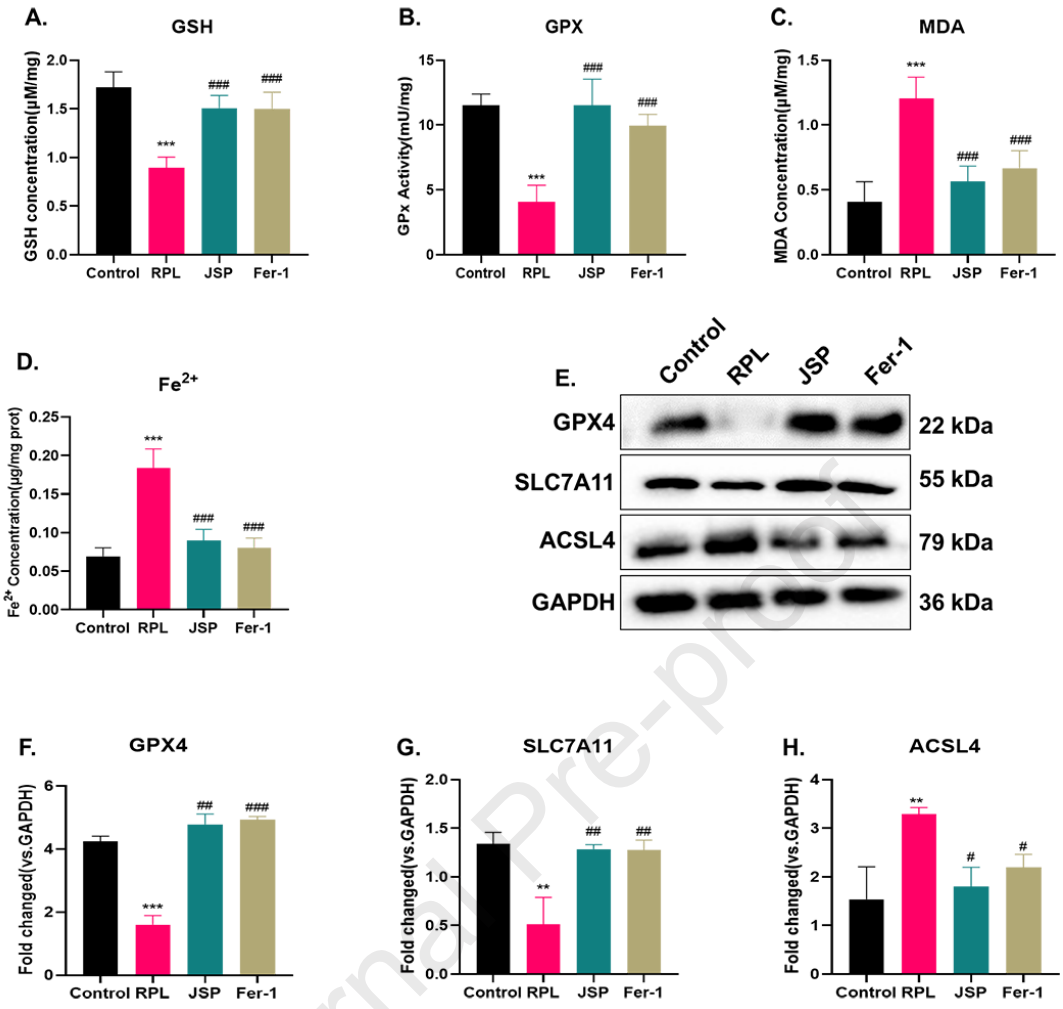

Figure 3. Both JSP and Fer-1 inhibited ferroptosis in RPL mice

(A-C) GSH content, GPX activity and MDA level of implantation sites in each group (n = 5 per group). (D) Fe^{2+} of implantation sites in each group was measured (n = 5 per group). (E) Western blot assay tested protein expressions of GPX4, SLC7A11 and ACSL4 of implantation sites in each group. (F-H) Corresponding quantitative histograms of (E) (n = 3 per group). $^{**}P<0.01$, $^{***}P<0.001$, compared with the control group; $^{\#}P<0.05$, $^{\#\#}P<0.01$, $^{\#\#\#}P<0.001$ compared with the RPL group.

To explore the functional role of ferroptosis related genes in RPL mice, the expression and localization of GPX4, SLC7A11 and ACSL4 in whole implantation sites were analyzed. Compared with JSP and Fer-1 groups, GPx4 and SLC7A11 expressions were descending, and ACSL4 expression was elevated in RPL group (**Figure 3E-H**). Similar protective effects of JSP and Fer-1 on RPL mice were shown in immunohistochemical

analysis (**Figure 4A-D).** Besides, the protein expressions of GPx4, SLC7A11, and ACSL4 mainly distributed in the labyrinth zone (LZ) and decidual basalis (DB), and partly distributed in the trophospongium (TS) (**Figure 4A**).

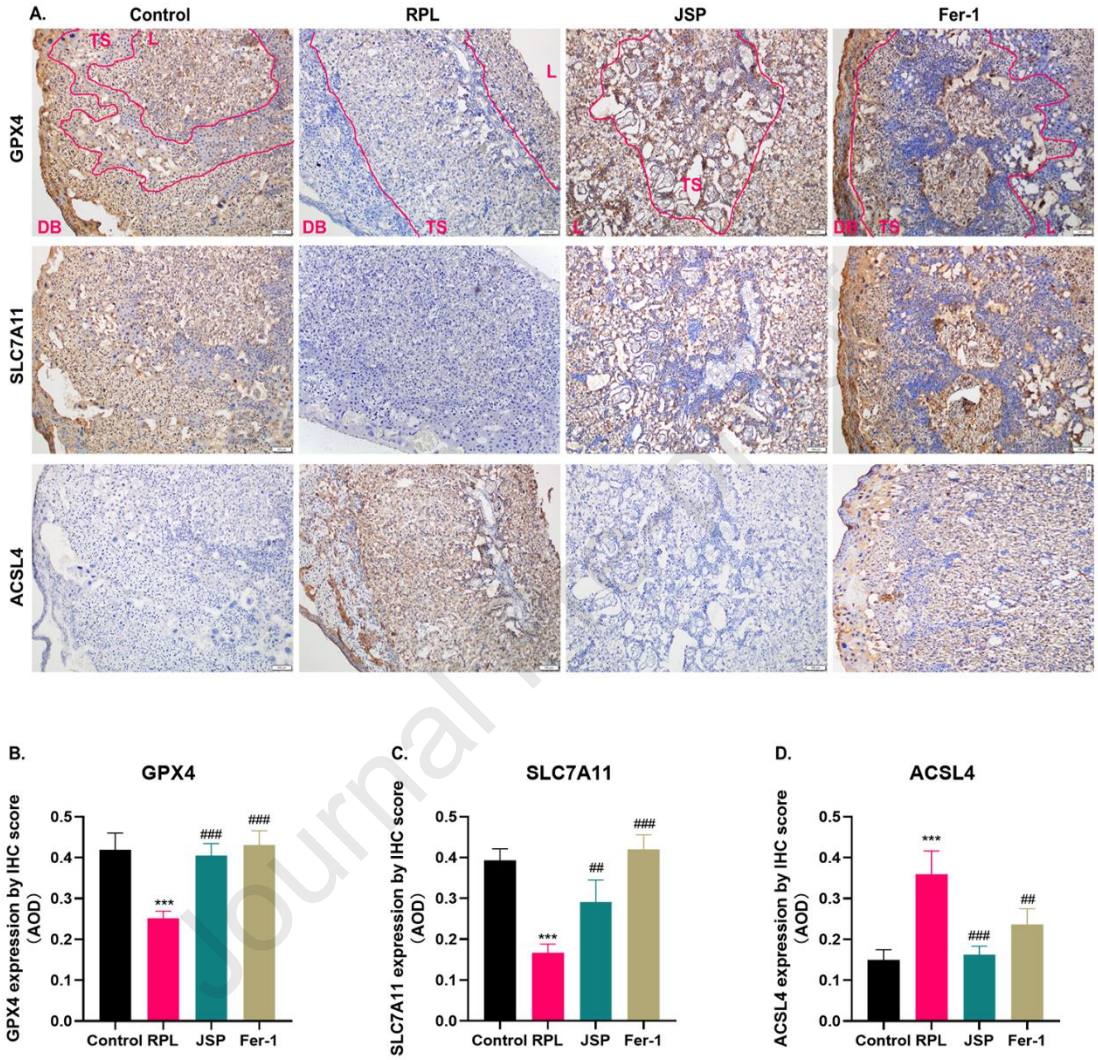

Figure 4. Immunohistochemical staining tested protein expressions of GPX4, SLC7A11 and ACSL4 in mice

(A) Representative images of GPX4, SLC7A11 and ACSL4 of implantation sites with immunohistochemical staining. Scale bar: 100 μm. (B-D) Relative immunohistochemical scores of GPX4, SLC7A11 and ACSL4 (n = 4 per group). Labyrinth zone (LZ); Decidual basalis (DB); Trophospongium (TS). $^{***}P<0.001$, compared with the control group; $^{\#\#}P<0.01$, $^{\#\#\#}P<0.001$ compared with the RPL group.

3.3. JSP suppressed cell death induced by RSL3

The CCK-8 assay was performed to analyze whether JSP rescued cell cytotoxicity

induced by RSL3 in HTR-8/SVneo cells. According to our previous study, 0.1μM RSL3 was an effective ferroptosis inducer for HTR-8/SVneo cells(Lai et al 2022). As shown in **Figure 5A,** 0.1 μM RSL3 induced cell damage in a time-dependent manner, and JSP obviously protected cell viability from exposure to RSL3 in dose-dependent manner. Besides, among the three different concentrations of JSP, both 10% and 15% JSP could almost completely reverse RSL3 induced cell damage. Meanwhile, the cytotoxicity of RSL3 injury on trophoblasts was inhibited by various concentrations of JSP **(Figure 5B)**. Compared to the control group**,** HTR-8/SVneo cell behaved thinner and the adhesion ability was worse in RSL3 group and JSP groups and restore cell morphology **(Figure 5C)**.

The invasion of trophoblasts is the key step of embryo implantation. Inadequate invasion may cause abnormal placental function, then lead to abortion(Huang et al 2022). According to the wound healing assay **(Figure 5D-E)**, the scratch recovery rate was obviously raised in JSP groups compared to the RSL3 group.

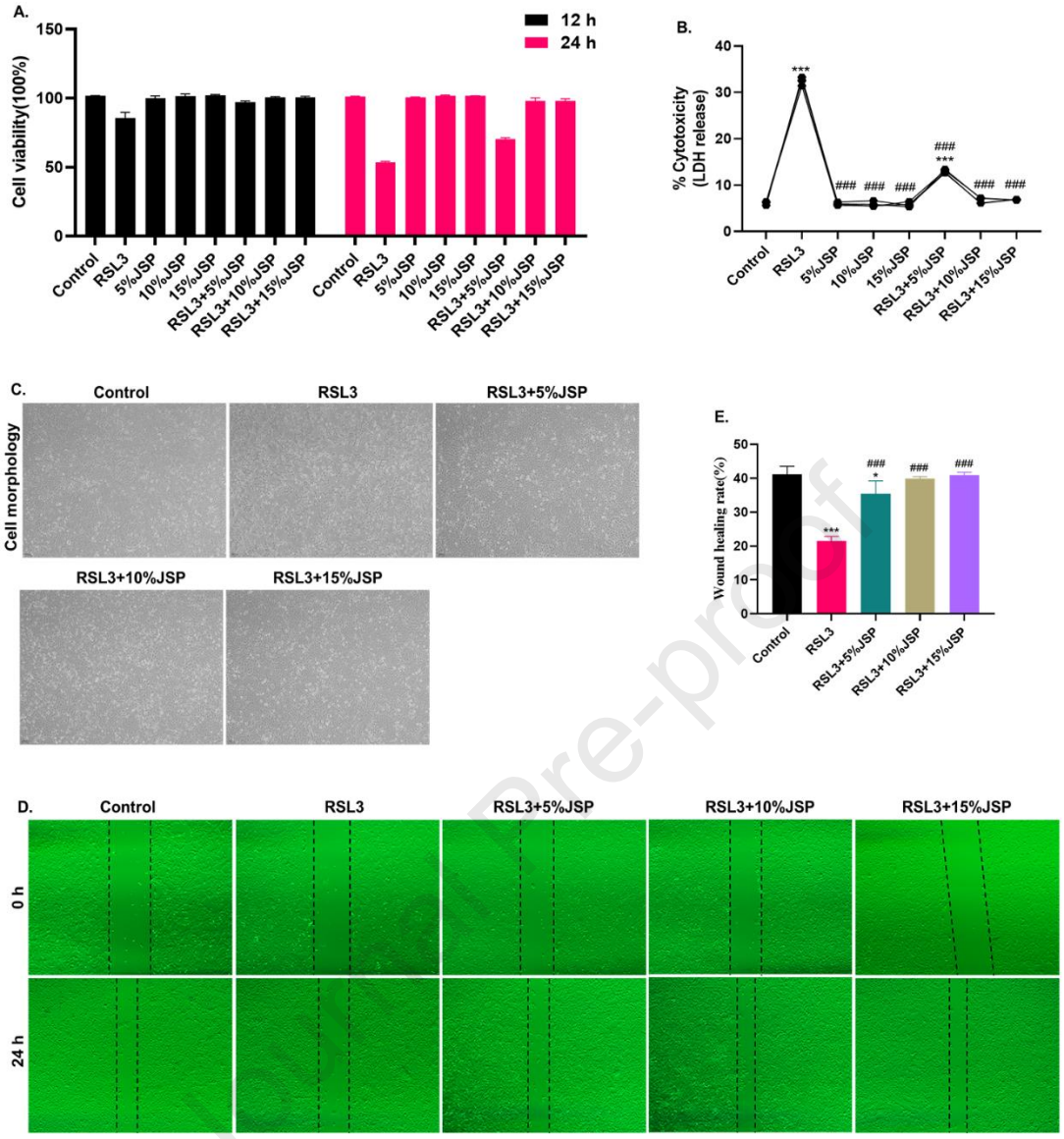

Figure 5. JSP saved cell death induced by RSL3 in HTR-8/SVneo cells

(A)CCK8 measured cell viability (n =5 per group). (B)Effects of different concentrations of JSP on RSL3-induced cytotoxicity. (C) Representative images of cell morphology after treatment with RSL3 or different concentrations of JSP. Scale bar: 100 μm. (D)The migration ability of HTR-8/SVneo cells was detected by wound healing assay and the representative images were taken at 0 h and 30 h. (E) The wound healing rates of cells are summarized (n = 6 per group). $^{***}P<0.001$, compared with the control group; $^{\#\#\#}P<0.001$ compared with the RSL3 group.

3.4. JSP inhibited RSL3 induced lipid peroxidation and iron deposition in HTR-8/SVneo cells

Excessive ROS and lipid peroxidation are considered the basic characteristics of

ferroptosis. GSH converts toxic lipid hydroperoxides into non-toxic lipid alcohols through enzymatic activity of GPXs, while MDA could reflect the degree of cell membrane damage as the end product of lipid peroxidation(Conrad & Pratt 2019). As shown in **Figure 6A-C**, RSL3 significantly reduced GSH content, GPX activity and raised MDA level, while all the JSP groups notably increased GSH and GPX contents and reduced MDA level. Next, the intracellular ROS was measured by DCFH-DA fluorescent probe. To supplement with 5%, 10% and 15% JSP notably decreased intracellular ROS (**Figure 6D, E**) in RSL3-administrated HTR-8/SVneo cells. Additionally, RSL3 generated excessive lipid ROS in the cell membrane, while 5%/10%/15% JSP inhibited the pathologic increase of lipid ROS **(Figure 6D).** The results above suggested that JSP effectively inhibited the lipid peroxidation process in ferroptosis.

The iron content is recognized as an important signal for indicating the degree of ferroptosis, and cellular labile Fe^{2+} levels were reflected by LIP level, so we investigated iron uptake and efflux by detecting LIP. According to FeRhoNox-1 probe, JSP resulted in a decrease in LIP level compared with the RSL3 group **(Figure 6D, F)**, which revealed that JSP suppressed iron aggregation.

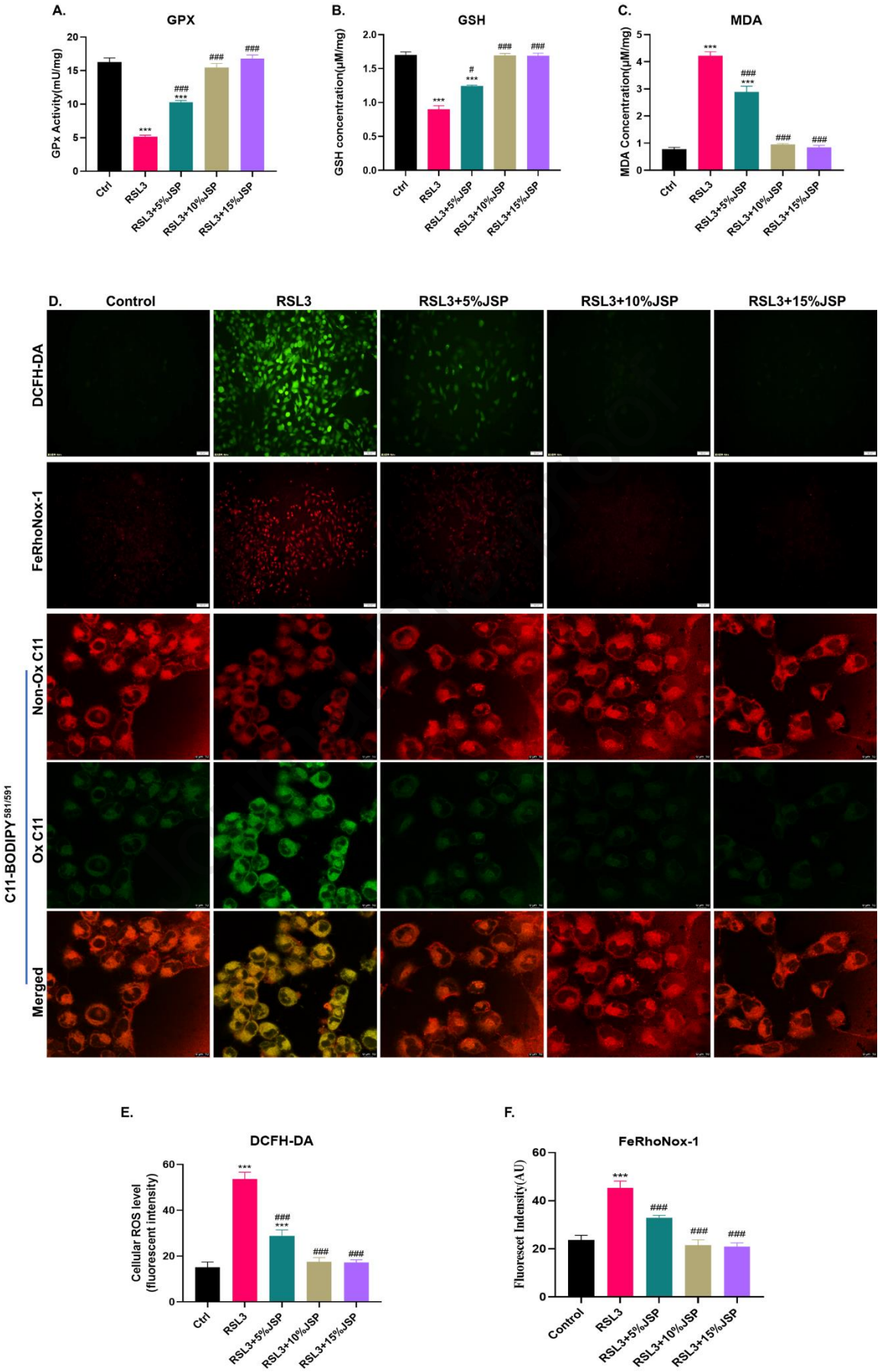
A.
GPX
GPx Activity(mU/mg)
B.
GSH
GSH concentration(μM/mg)
C.
MDA
MDA Concentration(μM/mg)
Ctrl
RSL3
RSL3+5%JSP
RSL3+10%JSP
RSL3+15%JSP
D.
Control
RSL3
RSL3+5%JSP
RSL3+10%JSP
RSL3+15%JSP
DCFH-DA
FeRhoNox-1
C11-BODIPY 581/591
Non-Ox C11
Ox C11
Merged
E.
DCFH-DA
Cellular ROS level (fluorescent intensity)
F.
FeRhoNox-1
Fluoreset Indensity(AU)
Control

411

Figure 6. JSP inhibited RSL3 induced lip peroxidation and iron deposition in HTR-8/SVneo cells

(A-C) GPX activity, GSH content and MDA levels were measured utilizing the corresponding detection kits. n = 3 per experiments. (D)Cellular ROS, LIP and membrane lipid ROS were measured via DCFH-DA probe, FeRhoNox-1 probe and C11-BODIPY $^{581/591}$ probe, respectively. Scar bar of DCFH-DA = 50 μm; scar bar of FeRhoNox-1 = 100 μm; scar bar of C11-BODIPY $^{581/591}$ = 10 μm. (E) The data of DCFH-DA were quantified by ImageJ software. n = 3 per experiment. (F) The data of FeRhoNox-1 were quantified by ImageJ software. n = 3 per experiment. $^{***}P<0.001$, compared to the control group; $^{###}P<0.001$ compared to the RSL3 group.

3.5. JSP reversed ferroptosis related protein expressions in HTR-8/SVneo cells

We further conducted western blotting assay to examined the protein expressions of GPx4, SLC7A11 and ACSL4. GSH is the main antioxidant in cells. SLC7A11 is the key of GSH synthesis(Koppula et al 2018) and GPx could utilize GSH to detoxify lipid peroxides(Chen et al 2021). ACSL4 is mainly responsible for the acylation of polyunsaturated fatty acids (PUFA)(Doll et al 2017). FTH1, known as ferritin, is a key member of the iron storage protein complex(Ouyang et al 2022). Ferroptosis-sensitive cells have reduced FTH1 expression compared to ferroptosis-resistant cells(Xie et al 2016). In comparison with RSL3 group (**Figure 7 A-D**), different concentrations of JSP groups significantly increased the expressions of GPx4 and FTH1, and decreased ACSL4 expression. Collectively, JSP could protect RSL3-induced lipid metabolic process. Additionally, among the three concentrations, 15% JSP exerted better in reversing ferroptosis related proteins. Hence, high concentration of JSP was administered in animal experiments.

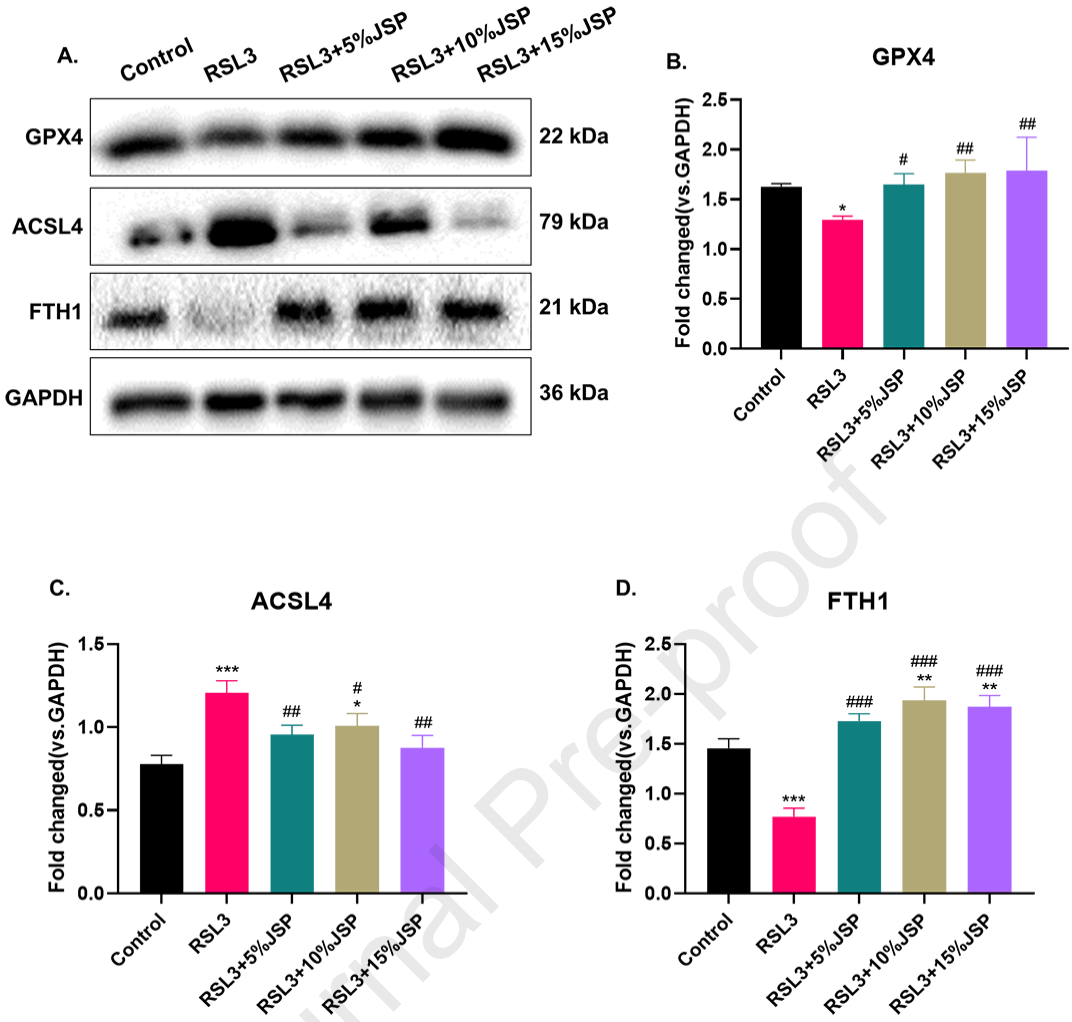

Figure 7. JSP reversed ferroptosis related protein expressions in HTR-8/SVneo cells

(A) Western blotting measured protein expression of GPx4, ACSL4 and FTH1 in HTR-8/SVneo cells. (B-E) Corresponding quantitative histograms of (A) (n = 3 per group). $^{*}P<0.05$, $^{**}P<0.01$, $^{***}P<0.001$, compared with the control group; $^{\#\#}P<0.01$, $^{\#\#\#}P<0.001$ compared with the RSL3 group.

4. Discussion

The decline of female fertility has become a key issue endangering global population security, and reproductive health is facing severe challenges. Recurrent abortion is a common problem in the field of reproductive medicine, affecting 2% - 5% of couples

around the world. However, the cause of half of RPL cases is still unclear, which makes its evidence-based diagnosis and treatment limited. The early stage of normal pregnancy requires a hypoxic environment, which has also been revealed to play an important role in blastocyst implantation, trophoblast differentiation and decidual development (Zhao et al 2021). Previous studies have manifested that the overactivation of ROS in the whole body and the placenta may induce RPL (Al-Sheikh et al 2019). Ferroptosis is driven by an accumulation of iron-dependent ROS and involves in the occurrence and development of various diseases such as cancer, kidney disease, nervous system disease. Excessive levels of ferroptosis were observed in the H_2O_2 induced cellular model of placental oxidative stress (Meihe et al 2021). Whether ferroptosis is related to the occurrence and development of RPL, or whether ferroptosis could treat RPL remain to be illuminated.

CBA/J mated DBA/2 has been widely utilized as an RPL model (Bai et al 2021). Firstly, we successfully established the RPL mouse model by mating female CBA/J mice with male DBA/2 mice. In the implantation sites of RPL mice, the indexes related to enhancing lipid peroxidation and iron deposition were significantly increased, revealing the existence of ferroptosis. The mechanism of introducing cysteine to synthesize GSH through cystine is the classic pathway when ferroptosis was first discovered. GPX could accelerate the conversion of GSH to oxidized glutathione and the conversion of harmful lipid hydroperoxides to non-toxic lipid alcohols. (Chen et al 2021). Therefore, GSH and GPX are generally used to reflect the antioxidant activity of the body. In the placenta of RPL mouse, we observed the decrease levels of GPX and GSH suggesting the failure of antioxidant mechanism in RPL. Consistent with clinical studies, previous studies have found that GSH activity in RPL women was lower than in healthy pregnancy (Mistry & Williams 2011). MDA is a classic index to analyze the degree of lipid peroxidation. Herein, increased MDA expression was observed in the RPL group revealing the superfluous accumulation of lipid peroxides. Hence, we extrapolated that excessive generation of ROS during RPL induced lipid peroxidation at the maternal-fetal interface which provided a foundation for triggering ferroptosis.

In the subsequent western blotting and immunohistochemistry experiments, the abnormal expressions of GPX4, SLC7A11 and ACSL4 further suggested that ferroptosis was involved in the pathological process of RPL. Ferroptosis is closely regulated by iron metabolism, GSH and GPX4 lipid repair system, and depends on a series of enzyme activity reactions (Stockwell 2022). SLC7A11 is the main subunit of cystine/glutamic acid reverse transport system (Xc^-) which imports cystine to build blocks for GSH. SLC7A11 limits the accumulation of lipid oxidation products and suppresses ferroptosis by maintaining the cellular levels of GSH (Lee & Roh 2022). As the key enzyme of fatty acid metabolism, ACSL4 enhanced PUFA synthesis in phospholipids which are prone to oxidation processes that cause ferroptosis (Tang et al 2021). Hence, the decreased expression of GPX4 and SLC7A11, and the increased expression of ACSL4 showed activation of ferroptosis in RPL mice. Besides, Fer-1 significantly inhibited the abortion rate of RPL. Fer-1 has been confirmed as a potent inhibitor of ferroptosis for its ability to impede the accumulation of lipid peroxidation (Zilka et al 2017). Therefore, we considered that the prevention of abortion by Fer-1 may be related to the restoration of antioxidant capacity of mice. Based on the above results, we believe that inhibiting ferroptosis may be the key to inhibit the pathological process of RPL and improve the pregnancy outcome.

Intriguingly, JSP effectively inhibited ferroptosis both in *vivo* and in *vitro* tests. It is universally known that modern therapy has limited effect in preventing RPL. Recently, TCM has gained popularity as a supplemental therapy to western medicine in the treatment of RPL (Li et al 2020). Some clinical studies have reported that TCM could improve pregnancy and promote the continuation of pregnancy(Li et al 2016), but the mechanism and efficiency of TCM in treating RPL are unclear. TCM holds that “Qi” and “Blood” are the basic pathological elements of RPL, and the deficiency of “Qi” and “Blood” in the kidney is the root to the disease. Hence the principle of TCM in treating RPL is correcting kidney deficiency. Shoutai Pill is commonly used in China for treating RPL because of its satisfied effect and high safety and reliability. Previous studies found that Shoutai Pill could prevent placental tissue damage and enhance

pregnancy outcomes by addressing the imbalance of placental tissue oxidative stress produced by DEHP (Jin et al 2020). JSP is obtained by optimizing the ratio after removing the animal drug ingredients (donkey-hide gelatin) in Shoutai pills. We found that RPL mice manifested more resorption embryos on the GD12.5 of pregnancy, compared with normal pregnant mice. JSP or Fer-1 had significant effects on inhibiting abortion rate and improving embryo quality, and there was no statistical difference between the two groups. JSP obviously increased the content of GSH and GPX, and inhibited the generation of MDA suggesting that JSP has the ability to prevent lipid peroxidation, which is similar to the effect of Fer-1. In addition, the enhanced expressions of GPX4 and SLC7A11, and the decreased levels of ACSL4 in the JSP group indicating that JSP could promote the production of glutathione and reduce lipid peroxidation. Consistent with *in vivo* experiments, JSP inhibited RSL3-induced iron deposition, intracellular ROS and lipid ROS production in HTR-8/SVneo cells. According to our knowledge, this is the first discovery that JSP could inhibit ferroptosis in RPL.

Iron regulation is another cornerstone of ferroptosis. Elevated iron level propagates lipid peroxidation by Fenton reaction, subsequently causes cell damage (Feng et al 2020). Fe^{2+} is kept in the cells in the form of the labile iron pool (Stockwell 2022). The content of Fe^{2+} in the implantation site of RPL mice was considerably higher than that in the control group, implying that the increase of intracellular free iron at the maternal-fetal interface was responsible for ferritin deposition. FTH1 chelate with iron ions to limit the size of the LIP which drive Fenton reaction (Yang et al 2022). *In vitro*, JSP inhibited LIP accumulation and enhanced FTH1 expression; *in vivo*, JSP controlled the excessive accumulation of LIP. The consumption of GSH not only affects the synthesis of GPX4, but also mobilizes Fe^{2+} for Fenton reaction. In this study, JSP not only inhibited iron accumulation, but also increased GSH content which suggested that JSP may inhibit the Fenton reaction by promoting the synthesis of GSH, thus preventing the proliferation of lipid peroxides and ultimately blocking ferroptosis. Iron demand increases during pregnancy and iron supplementation is

universally recommended for women throughout pregnancy (Zhang et al 2022). However, the benefits of preventive iron supplements for every pregnant woman are still controversial. Actually, compared with nongravid state, demands for iron in the first trimester are even lower (Zaugg et al 2022). Considering that RPL mainly occurs in the first trimester and is closely related to ferroptosis, this study also expressed concern about the suggestion of routine iron supplementation for pregnant women in the early pregnancy.

Normal activity and function of trophoblasts are the basis for maintaining pregnancy. 5%, 10% and 15% concentrations of JSP significantly improved the cell viability and reduced the cytotoxicity caused by RSL3. Besides, JSP groups promoted the invasiveness of trophoblasts. These results indicated that RSL3-induced functional damage of trophoblast could be recovered by JSP which further explains the protective effect of JSP on normal pregnancy.

CBA/J mated DBA/2 has been commonly used to establish an abortion prone mouse model, which induces pregnancy loss through immune rejection of fetus (Clark et al 1986), such as increased lymphocyte transport, enhanced complement deposition and activation of NK and T cells in maternal-fetal interface (Yadav et al 2016). Previous studies have found that ferroptosis played an important role in against immune tolerance. GPx4-decificient Treg cells manifested excessive accumulation of lipid peroxidation and underwent ferroptosis, then prohibiting immune tolerance(Xu et al 2021). Activated CD8 T cells have been reported to promote ferroptosis-specific lipid peroxidation (Wang et al 2019) and arachidonic acid (AA) cooperated with CD8 T cells (or IFN-γ) could induce ferroptosis through ACSL4 in tumor cells (Liao et al 2022). There exists a bright prospect to explore whether immune regulation is the potential mechanism of high expression of ferroptosis in the placenta of CBA/J × DBA/2 mice

induced RPL. Besides, Shoutai Pills has been reported to enhance the maternal-fetal immune tolerance through transforming Th1/Th2 cytokine towards Th2 bias(Lai et al 2010). Hence, in the subsequent experiments, it is necessary for us to explore whether JPS could regulate ferroptosis through immune mechanism.

This study suggested that JSP could inhibit ferroptosis, enhance cell proliferation and invasion abilities, and improve pregnancy outcomes. We believe that the multiple effects of JSP will provide promising clinical values for the treatment of RPL.

5. Conclusions

This study for the first time found that JSP effectively alleviated RPL via inhibiting ferroptosis, which provides an exciting new idea for the current dilemma of lacking RPL therapeutic strategies. However, the results presented here are limited in their applicability to humans because the experimental design's use of mice. It is mostly because mice and humans have different anatomy and physiology during pregnancy and delivery (mice have a bicornular uterus and a large nest). In order to fully understand the role of JSP in the pathophysiology of pregnancy, further clinical research and mechanisms of multiple components are needed.

Author contributions

Yuling Lai designed the experiments and wrote the manuscript; Yu Zhang and Huimin Zhang performed the animal experiments; Zhenyue Chen and Lihua Zeng prepared the decoction of JSP and performed the LC/MS analysis; Gaopi Deng helped perform the analysis with constructive discussions; Songping Luo and Jie Gao provided experimental ideas and were responsible for manuscript monitoring.

Declaration of competing interest

The authors declare that they have no known competing financial interests or personal

relationships that could have appeared to influence the work reported in this paper.

Acknowledgments

This work was supported by the National Natural Science Foundation of China (82274565), Education Bureau of Guangdong Province (2021ZDZX2033), the Department of Finance of Guangdong Province (2020B11111100003), Guangzhou Key Laboratory of Traditional Chinese Medicine for the Prevention and Treatment of Female Reproductive Disorders(202201020383), Training Project of Young Qihuang Scholars (Letter of Personnel Education Department of National Administration of Traditional Chinese Medicine [2022] No. 256).

References:

Al-Sheikh YA, Ghneim HK, Alharbi AF, Alshebly MM, Aljaser FS, Aboul-Soud M. 2019. Molecular and biochemical investigations of key antioxidant/oxidant molecules in Saudi patients with recurrent miscarriage. *EXP THER MED* 18:4450-60

Amer SRM. 2012. Evaluation and treatment of recurrent pregnancy loss: a committee opinion. *FERTIL STERIL* 98:1103-11

Aouache R, Biquard L, Vaiman D, Miralles F. 2018. Oxidative Stress in Preeclampsia and Placental Diseases. *INT J MOL SCI* 19

Atik RB, Christiansen OB, Elson J, Kolte AM, Lewis S, et al. 2018. ESHRE guideline: recurrent pregnancy loss. *HUMAN REPRODUCTION OPEN* 2018

Bai S, Huang B, Fu S, Zhu M, Hu L, et al. 2021. Changes in the Distribution of Intrauterine Microbiota May Attribute to Immune Imbalance in the CBA/J×DBA/2 Abortion-Prone Mice Model. *FRONT IMMUNOL* 12:641281

Beharier O, Tyurin VA, Goff JP, Guerrero-Santoro J, Kajiwara K, et al. 2020. PLA2G6 guards placental trophoblasts against ferroptotic injury. *Proc Natl Acad Sci U S A* 117:27319-28

Brannon PM, Taylor CL. 2017. Iron Supplementation during Pregnancy and Infancy: Uncertainties and Implications for Research and Policy. *NUTRIENTS* 9

Chen X, Li J, Kang R, Klionsky DJ, Tang D. 2021. Ferroptosis: machinery and regulation. *AUTOPHAGY* 17:2054-81

Clark DA, Chaput A, Tutton D. 1986. Active suppression of host-vs-graft reaction in pregnant mice. VII. Spontaneous abortion of allogeneic CBA/J x DBA/2 fetuses in the uterus of CBA/J mice correlates with deficient non-T suppressor cell activity. *J IMMUNOL* 136:1668-75

Conrad M, Pratt DA. 2019. The chemical basis of ferroptosis. *NAT CHEM BIOL* 15:1137-47

Dimitriadis E, Menkhorst E, Saito S, Kutteh WH, Brosens JJ. 2020. Recurrent pregnancy loss. *NAT REV DIS PRIMERS* 6:98

Dixon SJ, Lemberg KM, Lamprecht MR, Skouta R, Zaitsev EM, et al. 2012. Ferroptosis: An Iron-Dependent Form of Nonapoptotic Cell Death. *CELL* 149:1060-72

Doll S, Proneth B, Tyurina YY, Panzilius E, Kobayashi S, et al. 2017. ACSL4 dictates ferroptosis sensitivity by shaping cellular lipid composition. *NAT CHEM BIOL* 13:91-8

El Hachem H, Crepaux V, May-Panloup P, Descamps P, Legendre G, Bouet P. 2017. Recurrent pregnancy loss: current perspectives. *International journal of women's health* 9:331-45

Feng H, Schorpp K, Jin J, Yozwiak CE, Hoffstrom BG, et al. 2020. Transferrin Receptor Is a Specific Ferroptosis Marker. *CELL REP* 30:3411-23

Ferguson KK, Meeker JD, McElrath TF, Mukherjee B, Cantonwine DE. 2017. Repeated measures of inflammation and oxidative stress biomarkers in preeclamptic and normotensive pregnancies. *AM J OBSTET GYNECOL* 216

Fisher AL, Nemeth E. 2017. Iron homeostasis during pregnancy. *AM J CLIN NUTR* 106:1567S-1574S

Huang Z, Tang Z, Guan H, Leung W, Wang L, et al. 2022. Inactivation of Yes-Associated Protein Mediates Trophoblast Dysfunction: A New Mechanism of Pregnancy Loss Associated with Anti-Phospholipid Antibodies? *Biomedicines* 10

Jaslow CR, Carney JL, Kutteh WH. 2010. Diagnostic factors identified in 1020 women

with two versus three or more recurrent pregnancy losses. *FERTIL STERIL* 93:1234-43

Jin M, Chuan J, Shen Y, Fu P. 2020. [Effects of Shoutai pills on immune function and oxidative stress in pregnant rats with di(2-ethylhexyl) phthalate exposure]. *Nan fang yi ke da xue xue bao = Journal of Southern Medical University* 40:850-5

Koppula P, Zhang Y, Zhuang L, Gan B. 2018. Amino acid transporter SLC7A11/xCT at the crossroads of regulating redox homeostasis and nutrient dependency of cancer.:12

Koppula P, Zhuang L, Gan BY. 2021. Cystine transporter SLC7A11/xCT in cancer: ferroptosis, nutrient dependency, and cancer therapy. *PROTEIN CELL* 12:599-620

Lai M, You Z, Ma H, Lei L, Lu F, et al. 2010. [Effects of shoutai pills on expression of Th1/Th2 cytokine in maternal-fetal interface and pregnancy outcome]. *Zhongguo Zhong Yao Za Zhi* 35:3065-8

Lai M, You Z, Ma H, Lei L, Lu F, et al. 2010. [Effects of shoutai pills on expression of Th1/Th2 cytokine in maternal-fetal interface and pregnancy outcome]. *Zhongguo Zhong yao za zhi = Zhongguo zhongyao zazhi = China journal of Chinese materia medica* 35:3065-8

Lai Y, Zeng F, Chen Z, Feng M, Huang Y, et al. 2022. Shikonin Could Be Used to Treat Tubal Pregnancy via Enhancing Ferroptosis Sensitivity. *Drug Des Devel Ther* 16:2083-99

Lee DC, Romero R, Kim JS, Tarca AL, Montenegro D, et al. 2011. miR-210 Targets Iron-Sulfur Cluster Scaffold Homologue in Human Trophoblast Cell Lines Siderosis of Interstitial Trophoblasts as a Novel Pathology of Preterm Preeclampsia and Small-for-Gestational-Age Pregnancies. *AM J PATHOL* 179:590-602

Lee J, Roh JL. 2022. SLC7A11 as a Gateway of Metabolic Perturbation and Ferroptosis Vulnerability in Cancer. *Antioxidants (Basel)* 11

Li HF, Shen QH, Li XQ, Feng ZF, Chen WM, et al. 2020. The Efficacy of Traditional Chinese Medicine Shoutai Pill Combined with Western Medicine in the First Trimester of Pregnancy in Women with Unexplained Recurrent Spontaneous Abortion: A Systematic Review and Meta-Analysis. *BIOMED RES INT* 2020:7495161

Li L, Dou L, Leung PC, Chung TK, Wang CC. 2016. Chinese herbal medicines for

675 unexplained recurrent miscarriage. *Cochrane Database Syst Rev* 2016:D10568
676 Li Y, Liu X, Wang J, Liu Y, Teng H. 2016. [Effects of Shoutai Pill Containing Serum
677 on Bioactivity Behavior of Trophoblast Cells of Spontaneous Abortion Patients].
678 *Zhongguo Zhong xi yi jie he za zhi Zhongguo Zhongxiyi jiehe zazhi = Chinese journal*
679 *of integrated traditional and Western medicine* 36:586-91
680 Liao P, Wang W, Wang W, Kryczek I, Li X, et al. 2022. CD8(+) T cells and fatty acids
681 orchestrate tumor ferroptosis and immunity via ACSL4. *CANCER CELL* 40:365-78
682 Meihe L, Shan G, Minchao K, Xiaoling W, Peng A, et al. 2021. The Ferroptosis-NLRP1
683 Inflammasome: The Vicious Cycle of an Adverse Pregnancy. *Front Cell Dev Biol*
684 9:707959
685 Mistry HD, Williams PJ. 2011. The importance of antioxidant micronutrients in
686 pregnancy. *OXID MED CELL LONGEV* 2011:841749
687 Morita K, Ono Y, Takeshita T, Sugi T, Fujii T, et al. 2019. Risk Factors and Outcomes
688 of Recurrent Pregnancy Loss in Japan. *J Obstet Gynaecol Res* 45:1997-2006
689 Ouyang S, Li H, Lou L, Huang Q, Zhang Z, et al. 2022. Inhibition of STAT3-ferroptosis
690 negative regulatory axis suppresses tumor growth and alleviates chemoresistance in
691 gastric cancer. *REDOX BIOL* 52:102317
692 Sadeghi MR. 2016. ART Strategy for Treatment of Recurrent Pregnancy Loss: Isn't It
693 Better to Forget? *J Reprod Infertil* 17:191
694 Shintoku R, Takigawa Y, Yamada K, Kubota C, Yoshimoto Y, et al. 2017.
695 Lipoxygenase-mediated generation of lipid peroxides enhances ferroptosis induced by
696 erastin and RSL3. *CANCER SCI* 108:2187-94
697 Stockwell BR. 2022. Ferroptosis turns 10: Emerging mechanisms, physiological
698 functions, and therapeutic applications. *CELL* 185:2401-21
699 Su LJ, Zhang JH, Gomez H, Murugan R, Hong X, et al. 2019. Reactive Oxygen
700 Species-Induced Lipid Peroxidation in Apoptosis, Autophagy, and Ferroptosis. *OXID*
701 *MED CELL LONGEV* 2019
702 Tang D, Chen X, Kang R, Kroemer G. 2021. Ferroptosis: molecular mechanisms and
703 health implications. *CELL RES* 31:107-25

Taravati A, Tohidi F. 2018. Comprehensive analysis of oxidative stress markers and antioxidants status in preeclampsia. *TAIWAN J OBSTET GYNE* 57:779-90

Vaka VR, McMaster KM, Cunningham MW, Ibrahim T, Hazlewood R, et al. 2018. Role of Mitochondrial Dysfunction and Reactive Oxygen Species in Mediating Hypertension in the Reduced Uterine Perfusion Pressure Rat Model of Preeclampsia. *HYPERTENSION* 72:703-11

Vaughan JE, Walsh SW. 2002. Oxidative stress reproduces placental abnormalities of preeclampsia. *HYPERTENS PREGNANCY* 21:205-23

Wang W, Green M, Choi JE, Gijón M, Kennedy PD, et al. 2019. CD8(+) T cells regulate tumour ferroptosis during cancer immunotherapy. *NATURE* 569:270-4

Xiaoli H, Dongying W, Jie G, Songping L. 2020. Effect of modified Shoutai Pills on IL-17 in mice model of spontaneous abortion due to kidney deficiency. *World Journal of Integrated Traditional and Western Medicine* 15:292-5

Xie Y, Hou W, Song X, Yu Y, Huang J, et al. 2016. Ferroptosis: process and function. *CELL DEATH DIFFER* 23:369-79

Xu C, Sun S, Johnson T, Qi R, Zhang S, et al. 2021. The glutathione peroxidase Gpx4 prevents lipid peroxidation and ferroptosis to sustain Treg cell activation and suppression of antitumor immunity. *CELL REP* 35:109235

Yadav AK, Chaudhari H, Shah PK, Madan T. 2016. Expression and localization of collectins in feto-maternal tissues of human first trimester spontaneous abortion and abortion prone mouse model. *IMMUNOBIOLOGY* 221:260-8

Yang H, Zhang X, Ding Y, Xiong H, Xiang S, et al. 2022. Elabela: Negative Regulation of Ferroptosis in Trophoblasts via the Ferritinophagy Pathway Implicated in the Pathogenesis of Preeclampsia. *CELLS-BASEL* 12

Yang XT, Xu P, Zhang FM, Zhang L, Zheng YX, et al. 2018. AMPK Hyper-Activation Alters Fatty Acids Metabolism and Impairs Invasiveness of Trophoblasts in Preeclampsia. *CELL PHYSIOL BIOCHEM* 49:578-94

Yuexi Z, Qingying Y, Songping L, Jie G. 2021. Effect of Jianwei Shoutai Pill on FOXO3 and PR Protein Expression in Decidua of Spontaneous Abortion Model Mice.

J TRADIT CHIN MED 04:335-40

Zaugg J, Solenthaler F, Albrecht C. 2022. Materno-fetal iron transfer and the emerging role of ferroptosis pathways. *BIOCHEM PHARMACOL* 202:115141

Zhang H, He Y, Wang JX, Chen MH, Xu JJ, et al. 2020. miR-30-5p-mediated ferroptosis of trophoblasts is implicated in the pathogenesis of preeclampsia. *REDOX BIOL* 29

Zhang L, Wang S, Ma Y, Song Y, Li D, et al. 2023. Shoutai Wan regulates glycolysis imbalance at the maternal-fetal interface in threatened abortion mice. *J ETHNOPHARMACOL* 312:116502

Zhang Y, Lu Y, Jin L. 2022. Iron Metabolism and Ferroptosis in Physiological and Pathological Pregnancy. *INT J MOL SCI* 23

Zhao H, Wong RJ, Stevenson DK. 2021. The Impact of Hypoxia in Early Pregnancy on Placental Cells. *INT J MOL SCI* 22

Zilka O, Shah R, Li B, Friedmann AJ, Griesser M, et al. 2017. On the Mechanism of Cytoprotection by Ferrostatin-1 and Liproxstatin-1 and the Role of Lipid Peroxidation in Ferroptotic Cell Death. *ACS Cent Sci* 3:232-43

Figure legends

Figure 1. Chemical characterization of JSP drug-containing serum and decoctions using HPLC.

(A) Chemical characterization of mediated serum of JSP. (B) Chemical characterization of JSP decoctions.

Figure 2. Both JSP and Fer-1 attenuated pregnancy loss in CBA/J×DBA/2 mice

(A) Representative images of embryos in each group. Arrows indicated resorbed embryos. (B) Resorption rate in each group (n = 10 per group). (C) Abortion rate in each group (n = 10 per group). (D-F) Comparison of uterus weight, decidual weight and body weight in each group (n = 10 per group). G. Representative images of the placenta tissue by TUNEL staining. (H) Quantification of apoptosis by TUNEL staining (n =4 per group). Scale bar: 100 μm. $^{**}P<0.01$, $^{***}P<0.001$, compared with the control

group; $^{\#}P<0.05$, $^{\#\#}P<0.01$, $^{\#\#\#}P<0.001$ compared with the RPL group.

Figure 3. Both JSP and Fer-1 inhibited ferroptosis in RPL mice

(A-C) GSH content, GPX activity and MDA level of implantation sites in each group (n = 5 per group). (D) Fe^{2+} of implantation sites in each group was measured (n = 5 per group). (E) Western blot assay tested protein expressions of GPX4, SLC7A11 and ACSL4 of implantation sites in each group. (F-H) Corresponding quantitative histograms of (E) (n = 3 per group). $^{**}P<0.01$, $^{***}P<0.001$, compared with the control group; $^{\#}P<0.05$, $^{\#\#}P<0.01$, $^{\#\#\#}P<0.001$ compared with the RPL group.

Figure 4. Immunohistochemical staining tested protein expressions of GPX4, SLC7A11 and ACSL4 in mice

(A) Representative images of GPX4, SLC7A11 and ACSL4 of implantation sites with immunohistochemical staining. Scale bar: 100 μm. (B-D) Relative immunohistochemical scores of GPX4, SLC7A11 and ACSL4 (n = 4 per group). Labyrinth zone (LZ); Decidual basalis (DB); Trophospongium (TS). $^{***}P<0.001$, compared with the control group; $^{\#\#}P<0.01$, $^{\#\#\#}P<0.001$ compared with the RPL group.

Figure 5. JSP saved cell death induced by RSL3 in HTR-8/SVneo cells

(A)CCK8 measured cell viability (n =5 per group). (B)Effects of different concentrations of JSP on RSL3-induced cytotoxicity. (C) Representative images of cell morphology after treatment with RSL3 or different concentrations of JSP. Scale bar: 100 μm. (D)The migration ability of HTR-8/SVneo cells was detected by wound healing assay and the representative images were taken at 0 h and 30 h. (E) The wound healing rates of cells are summarized (n = 6 per group). $^{***}P<0.001$, compared with the control group; $^{\#\#\#}P<0.001$ compared with the RSL3 group.

Figure 6. JSP inhibited RSL3 induced lip peroxidation and iron deposition in HTR-8/SVneo cells

(A-C) GPX activity, GSH content, MDA and SOD levels were measured using the corresponding detection kits. n = 3 per experiments. (D) Cellular ROS, LIP and membrane lipid ROS were measured via DCFH-DA probe, FeRhoNox-1 probe and C11-BODIPY $^{581/591}$ probe, respectively. Scar bar of DCFH-DA = 50 μm; scar bar of

FeRhoNox-1 = 100 μm; scar bar of C11-BODIPY $^{581/591}$ = 10 μm. (E) The data of DCFH-DA were quantified by ImageJ software. n = 3 individual experiments. (F) The data of FeRhoNox-1 were quantified by ImageJ software. n = 3 individual experiments. $^{***}P<0.001$, compared with the control group; $^{###}P<0.001$ compared with the RSL3 group.

Figure 7. JSP reversed ferroptosis related protein expressions in HTR-8/SVneo cells

(A) Western blotting measured protein expression of GPx4, ACSL4 and FTH1 in HTR-8/SVneo cells. (B-E) Corresponding quantitative histograms of (A) (n = 3 per group). $^{*}P<0.05$, $^{**}P<0.01$, $^{***}P<0.001$, compared with the control group; $^{##}P<0.01$, $^{###}P<0.001$ compared with the RSL3 group.

Highlights

- RPL mice behaved ferroptosis activation
- JSP could improve pregnancy outcomes in RPL mice
- JSP inhibited ferroptosis both in RPL mice and in RSL3-induced trophoblasts.

Declaration of interests

☑ The authors declare that they have no known competing financial interests or personal relationships that could have appeared to influence the work reported in this paper.

☐The authors declare the following financial interests/personal relationships which may be considered as potential competing interests: